

EIT & EUV BRIGHTPOINTS OVER THE SOHO MISSION SO FAR

Scott W. McIntosh⁽¹⁾ and Joseph B. Gurman⁽²⁾

⁽¹⁾Southwest Research Institute, Department of Space Studies, 1050 Walnut Street, Suite 400, Boulder, CO 80302, USA

⁽²⁾NASA Goddard Space Flight Center, Mail Code 682.3, Greenbelt, MD 20771, USA

ABSTRACT

We discuss early results derived from an algorithm that automates the detection, cataloging, and analysis of Extreme-ultraviolet (EUV) “Bright Points” (BP) from nearly eight years of data acquired by the Extreme-ultraviolet Imaging Telescope (EIT) on the *Solar and Heliospheric Observatory* (SOHO). In particular, we describe the temporal and spatial variations of the 1.3×10^8 EUV BPs observed by SOHO to date.

1. INTRODUCTION

We present diagnostics and early results from the ongoing development of an algorithm for the automatic cataloging and analysis of multiple wavelength observations of one of the solar corona’s most ubiquitous features, “bright points” (see the first references by Vaiana *et al.* 1970, Golub *et al.* 1974 and the review by Harvey 1997). The coronal Bright Point (BP), observed at X-Ray or Extreme-ultraviolet (EUV) wavelengths, has been associated with small, bipolar magnetic fields in the photosphere (e.g., Harvey *et al.* 1994b; Pawal 1999; Sattarov *et al.* 2002), sites of local magnetic reconnection in the corona (e.g., Harvey *et al.* 1994a; Shimojo & Shibata 1999; Kankelborg & Longcope 1999; Brown *et al.* 2002) and have been used extensively as a marker of solar differential rotation in the corona (see, for example, Brajsa *et al.* 2001 and other work by the same author). We will show that our ongoing, archival investigation of BPs is relatively straightforward but yields important information about behavior of the coronal plasma and its connection to the photosphere on multiple, physically important spatial and temporal scales.

It is presumed that X-Ray and EUV BPs arise by the same means and are largely similar in spatial extent (~ 2 -5Mm in diameter) and have the same (roughly) isotropic spatial distribution over the solar disk. The key factor differentiating the two is the number of bright points detected; apparently, this is due largely to the temperature sensitivity of the image being analyzed. The Soft X-Ray Telescope (SXT) of Yohkoh (e.g., Acton *et al.* 1992) was most sensitive to plasma temperatures between 3 and 10 MK, while SOHO’s Extreme-ultraviolet Imaging Telescope (EIT; Delaboudinière *et al.* 1995) has three pass bands with peak sensitivities at wavelengths around 171Å; 195Å and 284Å that are dominated by lines from species with equilibrium ionization concentrations characteristic of 0.9 - 1.0, 1.5 and 2.0 MK respectively. Using the EIT data archive we are able quantitatively to assess the appearance of BPs in all three temperature ranges from the launch of SOHO to the present.

From the start of 1997 EIT has almost continually observed the solar corona in those three coronal passbands, usually at a pixel scale of 2.6 arcseconds, on two primary timescales:

- “Synoptic” observations of the corona at a cadence of 6 hours. There are some 12,000+ images of this type per pass-band to date in the EIT archive.
- “CME watch” observations that comprise of one image every 12 minutes. These observations have been largely performed using the 195Å pass-band and there are more than 350,000 images of this type in the EIT archive to date.

The analysis of the synoptic set of observations allows us to investigate the appearance of BPs with temperature and the relative contribution they make to the EUV emission of the corona at each temperature. We can also compare the detected synoptic BPs with individual features on the solar disk, like small bipolar magnetic regions. The CME watch dataset can be exploited to study the coordinates, paths taken and lifetimes of individual BPs; these paths can then be used to study moving, quickly-varying, structures in the solar atmosphere like filaments. Similarly, the CME watch dataset can be used to infer maps of coronal differential rotation from the BP paths. Such maps can then be readily compared to their photospheric counterparts. Clearly, there is a lot of physical information in the EIT image archive that is not easy to extract in a reasonable time without an automated approach.

Over 1.3×10^8 EUV BPs have been identified in individual EIT images and cataloged. (This large figure does not factor in the lifetimes of those BPs. Using our tracking algorithm, we have followed more than 5×10^6 BPs over multiple images.) In the 195Å CME watch dataset from January 1997 to date, of which some 97% (within $0.6 R_{\odot}$) are associated with small magnetic bipoles (Harvey *et al.* 1993, 1994a, 1994b; Harvey 1997 and more references by the same authors). By monitoring the number and location of quiet-Sun BPs in this fashion, we can draw some preliminary conclusions about the behavior of BPs in the EIT data archive:

- There is a very weak dependence of the quiet-Sun BP number with the solar cycle; with possible double peaks in 2001 and 2003.
- This dependence would appear to be contradicted by the fact that the quiet-Sun BPs are uniformly distributed over the solar disk throughout this period,

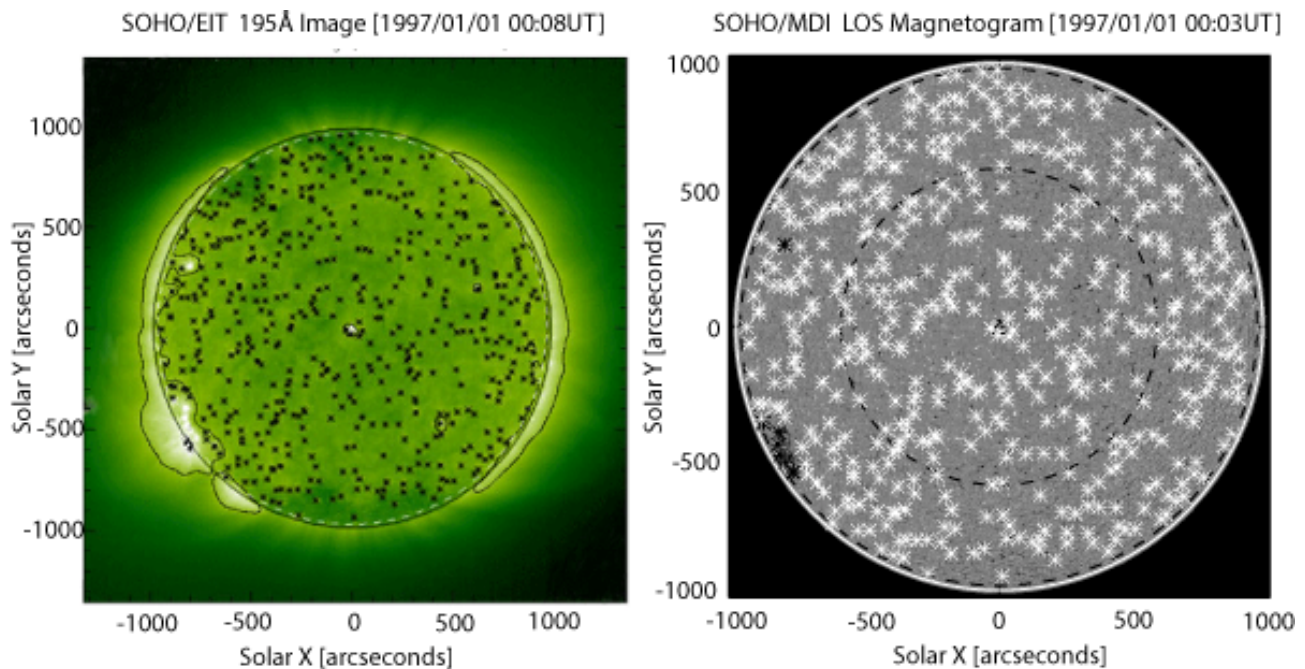


Figure 1. SOHO/EIT 195Å image (left) and SOHO/MDI line-of-sight magnetogram (right) from January 1, 1997. The outermost dashed line shows the $0.95R_{\odot}$ boundary of the detection algorithm. In the left panel the closed solid black contours designate areas that have background intensities above two-thirds of the mean value of the image; these contours designate active regions. The locations of the detected bright points are shown as asterisks (black: quiet-Sun - white: active region). In the right panel the inner dashed line designates the $0.60R_{\odot}$ boundary and the BP color identification is reversed.

and show little correlation with the equatorial migration of the activity belts over the same period.

- There is a strong dependence in the number of BPs detected with the pass band with which we are observing; typically the “coolest” EIT pass band (171Å; Fe IX/X) has approximately 100 more BPs than are present in the “hottest” pass band (284Å; Fe XV) at a given time. This simple fact indicates a temperature dependence in the generation mechanism of BPs, but we note that speculation on this point is beyond the scope of this paper.
- These are relatively simple diagnostics; when the BP information is placed in a simple query database we can then track individual BPs and monitor their lifetimes from creation to extinction. Although it appears that the lifetimes of quiet-Sun BPs do not vary significantly with time, that of BPs originating in active regions appear to slowly decay in the rising phase of the solar cycle, however we must note that this lengthy analysis is only complete until the end of 2000.

In the following sections we will discuss the BP detection algorithm itself (Sect. 2.) and the scientific analysis permitted as a simple by product of its application (Sect. 3.). In the final section (Sect. 4.1) we will discuss the next step; application of the outlined BP detection algorithm and database to the next generation of EUV im-

agers, but especially those on the Solar Dynamics Observatory (SDO).

2. THE DETECTION ALGORITHM

A great deal of research has been carried out on the topic of automated X-Ray BP detection from Yohkoh SXT images in recent years (e.g., Hara & Nakakubo-Morimoto, 2003). Likewise, Brajsa and colleagues (e.g., Brajsa *et al.* 2002) have developed a method of EUV BP detection in SOHO EIT images. The BP detection algorithm we propose (McIntosh & Gurman 2004) is a variant of the former, written in the Interactive Data Language (IDL), which exploits certain aspects of the latter and consists of the following recipe:

1. Take the raw EIT FITS file and perform the standard reduction steps outlined in the EIT User Guide. These steps involve dark current subtraction; degrading; filter normalization; exposure normalization; response correction; removal of vignetting and stray light.
2. Perform an additional step taken to further reduce the visibility of the grid pattern on the resulting images following poor removal in Step 1¹. The grid is

¹More information on the grid and this degrading tool will be provided in McIntosh & Gurman (2004).

then eventually responsible for a regular pattern of (over-)detected BPs that are coincident with its vertices. We use the *ridgelet* method (combination of Radon and Wavelet transforms; Do & Vetterli 2003) to isolate the grid pattern in phase space, remove its residual, and the artifact BPs from the image.

3. Remove the remaining bright spikes (predominantly cosmic-rays) in the data with a two-dimensional (15 x 15 pixel) median filter. This filtering process is important for estimating the background intensity of EUV for step 4.
4. Form an image of the EUV background intensity (I_{back}) from data (I_{image}) using 25×25 pixel box-car smoothing. To estimate the intensity of enhanced EUV regions (I_{diff}), subtraction of I_{back} from I_{image} is done: $I_{diff} = I_{image} - I_{back}$. Since there is significant EUV brightening around and above the limb (where the line-of-sight optical length is large) we limit the BP search area to be within a circle with radius of $0.95 R_{\odot}$.
5. Calculate the noise level (ΔI_{back}) of the background data I_{back} from the EUV photon statistical noise ΔI_{ph} (Poisson counting statistics; $I_{ph} = \sqrt{I_{image}}$), dark noise ΔI_{dark} , noise of visible stray light data ΔI_{stray} , as $\Delta I_{back} = [\Delta I_{ph}^2 + \Delta I_{dark}^2 + \Delta I_{stray}^2]^{1/2}$. The dark noise error is estimated from the ratio of subsequent dark images and the stray light error is computed in the EIT reduction package. We anticipate that the counting errors are dominant in this calculation.
6. Estimating the significance of I_{diff} we calculate the “deviation” image: $\sigma = I_{diff} / \Delta I_{back}$. We then define a BP candidate as a region in this image where σ exceeds 3. In this process extremely small and large bright areas cannot be rejected and so we have to add some restrictions for BP shape and size.
7. We regard a group of spatially neighbor pixels that satisfy Step 6 as a single BP and we must differentiate between them. We use the following BP shape selection rules:
 - a) The ratio of horizontal width to vertical width of BP shall be in a range of 0.4 - 2.5. This eliminates very large conglomerate points satisfying Step 6.
 - b) The BP shall occupy more than 40% of the product of its horizontal and vertical widths. This rule eliminates the smallest, spike-like, BPs.
8. Once detected, we number the BP and make an entry in a database constructed with a simple, Open Source, multi-platform-compatible database management code (MySQL), and store the basic quantities of the BP, such as location, area, and area integrated intensity.

Figure 1 shows the application of the BP detection algorithm to and EIT 195Å image (left panel) from January

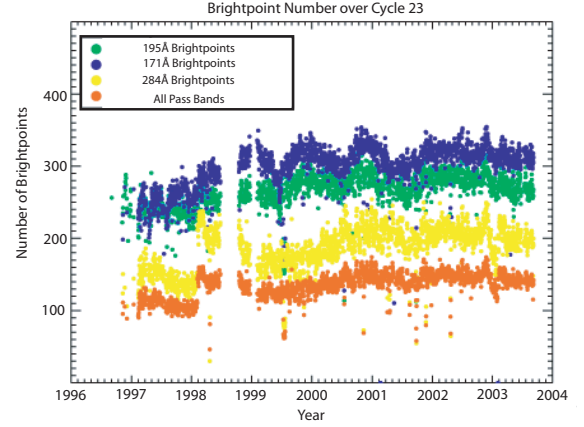


Figure 2. Variations of EUV Quiet-Sun Bright Point number from 1996 to 2004. These BP numbers were obtained from the SOHO/EIT four times daily synoptic observations and each dot represents the daily average number of BPs. The orange points indicate the number of BPs that are coincident in all three EIT coronal pass bands images at any one time.

1, 1997. The detected BPs are shown as asterisks (black; quiet-Sun - white; active region). As a contrast, we also show, in the right panel, the overlay of the detected BPs on the SOHO Michelson Doppler Imager (MDI; Scherrer *et al.* 1995) line-of-sight magnetogram. We note that 118 of the 125 BPs (within 60% of R_{\odot} ; inside the inner black dashed circle) are associated with small photospheric magnetic dipoles.

To quantify the temporal behavior of the BPs present in the database we must perform the accurate “mapping” of one image’s BPs to those of the next. This mapping procedure explicitly allows the decoupling of different BP timescales and thus provide evidence to investigate the physical mechanisms that are likely responsible for the production of BPs. To this end we have written “wrapping” algorithms for the database that continually monitor the state of the present image and compare it to the previous one to automatically connect the pairs of images and the BPs identified therein. This is through the application of a “fuzzy” photospheric differential rotation² scheme based on that detailed by Newton & Nunn (1951).

3. SUBSEQUENT BP ANALYSIS

There is a wealth of scientific understanding that can be made from the simple examination of the BP database. In this section we will demonstrate some of the very simple scientific diagnostics that are outlined above and will be readily available from the BP database. These diagnostics will probe a temporal domain that spans from minutes to years and a spatial domain that spans from the resolution of the observations to hundreds of megameters. These

²The “fuzzy” adaptation of the photospheric rotation allows for a little difference, or slip, between the corona and photosphere.

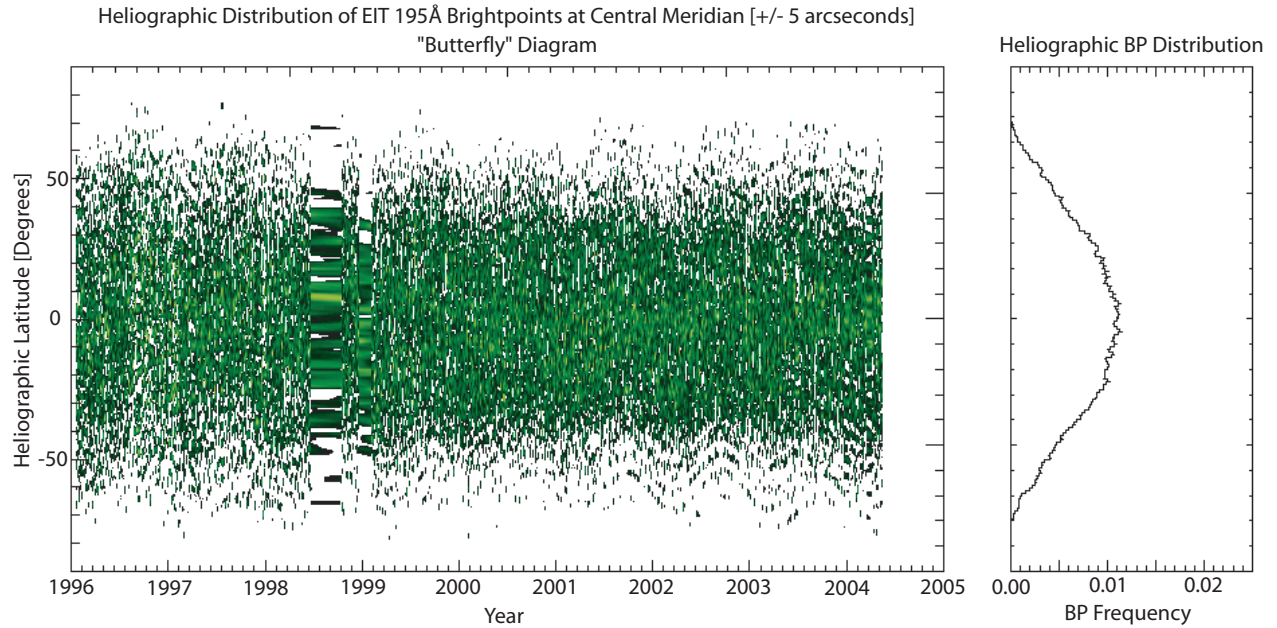


Figure 3. Distribution (number density) of the heliographic latitudes of quiet-Sun BPs that are visible in a narrow region (± 5 arcseconds) about the solar central meridian in 195\AA EIT synoptic images from 1996 through 2004; the large part of solar cycle 23.

diagnostics will not suffer from the statistics of small-numbers. From Fig. 2 and the work of Hara & Nakakubo-Morimoto (2003), we would expect many more than 180 BPs to be present in the coronal plasma in any one EIT image, over the course of a day (~ 120 images at a 12 minute cadence) there will be more than 21600 individual BPs detected; over eight years this number would be above 10^7 . Of course, not all BPs are truly individual and many of them track across the solar disk for tens of hours to days. Likewise, some of the detected BPs in any image will be much shorter-lived.

With the mapping wrapper algorithms in place we can discuss two particular varieties of BP diagnostic that can be recovered from the database:

- Variation diagnostics. Over scales of tens of minutes to years we can easily look at the number of BPs present in any image and their spatial distribution. These diagnostics are useful when looking for likely variations of BP number over the solar magnetic cycle, for example, providing evidence of direct physical connection between coronal processes and those from dynamo interactions in the solar interior. Likewise, on smaller timescales (minutes to hours) we can investigate the appearance and variation of BP numbers and locations with individual solar features (coronal holes, filaments, etc) and identify BP appearance with regions of possible local magnetic reconnection in the solar atmosphere. The latter is particularly important when we can detect BPs across many (wavelengths) temperatures in the solar atmosphere (e.g., for EIT at the synoptic cadence).

- Motion diagnostics. As BPs are tracked over the Sun's rotation period of 28 days we can construct maps of coronal differential rotation (cf. Brajsa *et al.* 2001). These will be easily to compare to their photospheric counterpart and their variation from one solar rotation to the next will be simple to assess. Using these maps we can investigate the "stiffness" of the corona (or difference in coronal rotation) relative to that of the photosphere. We can also measure the lifetimes of individual BPs directly and investigate whether or not their lifetimes vary as a function of where they occur in the atmosphere (e.g., in or near to a coronal hole or filament). Similarly, we will be able to look at potential variations of the BP lifetime over fixed temporal scales over the solar magnetic cycle; any possible variation in BP lifetimes would likely point to the mechanism by which energy is injected into the corona, say, for example the local reconnection rate (c.f. Shimojo & Shibata 1999; Kankelborg & Longcope 1999).

A number of useful diagnostics can be recovered from the automated detection and cataloging of EUV bright points in the *SOHO* archive in this manner, simply as a byproduct of the accurate detection and tracking process. In the following subsections we briefly illustrate some diagnostics on the database of EIT BPs.

3.1 BP Number Variation with Time and Space

By detecting and cataloging the properties of individual BPs present in each EUV image we can monitor the spectral, spatial and temporal variations in the total BP num-

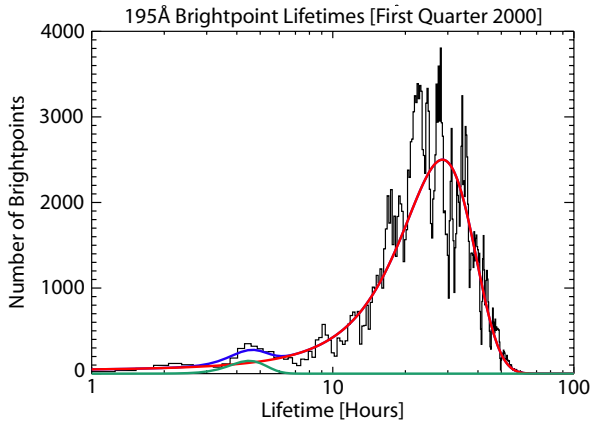


Figure 4. Accumulated statistics of BP lifetimes; the instance shown is for the first three months of 2000. Clearly there is a bimodal distribution between the active region and quiet-Sun BPs.

ber throughout the *SOHO* archive. Fig. 2 shows an example application of the daily mean quiet-Sun BP number variation from the EIT synoptic observations from late in 1996 to October of 2003. There are four synoptic images taken by EIT at regular six-hour intervals, in EIT’s three coronal pass-bands. From the dots corresponding to BPs detected in the coolest (blue 171Å; sensitive to Fe IX/X at 1MK) to those from the hottest (yellow 284Å; Fe XV at 3MK), we can see that there is a significant difference in the number of BPs detected on each day and over the seven plus years of observations considered. Hara & Nakakubo-Morimoto (2003) found that there were, on average, 150 quiet Sun X-Ray BPs (with an increase of ~ 100 in active regions near solar maximum in 2001). The similarity in the number of BPs detected at 5 MK with SXT by Harvey *et al.* (1993) and Hara & Nakakubo-Morimoto (2003), and the number we find in Fe XV 284Å represents a good consistency check of our BP detection method. The fact that we see this consistency in the hotter coronal plasma but an increasing BP number in the cooler coronal plasma sampled at 171Å and 195Å hints at a strong temperature dependence of the BP production mechanism or radiative dissipation.

3.2 Tracking BPs: BP Lifetimes

Employing a simple algorithm on the BP database we are able to “link” the BPs in a chain from one image to the next, and so on; from creation to extinction monitoring their lifetimes. Of course, monitoring the progression of BPs across the disk allows us to correlate their appearance with prominent solar features (coronal holes, filaments, etc) and to investigate the latitudinal (differential) dependence of coronal rotation compared to that of the photosphere; using the three EUV passbands we can investigate the differences with temperature as well. Likewise, by carefully studying the variations in the distributions of BP timescales we will be able to look at variations in coronal energy deposition rate over relatively short timescales and as an effective function of tempera-

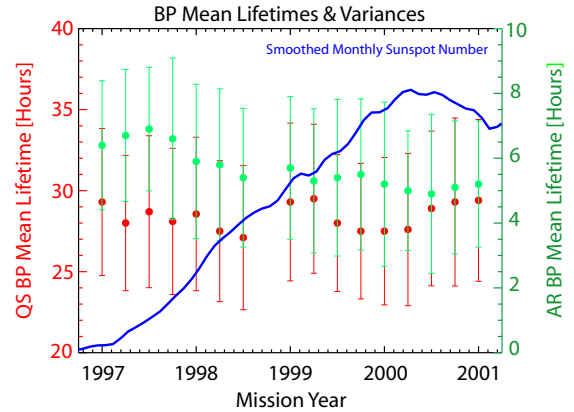


Figure 5. From the first quarter of 1997 until the last quarter of 2000 we have tracked and monitored the lifetimes of BPs. We show the variation in the mean quiet-Sun (red) and active region (green) BP lifetimes derived from distributions like those presented in Fig. 4. As a solar cycle reference we also show (blue) the smoothed sunspot number.

ture in the atmosphere (cf. Harvey *et al.* 1993; Kankelborg & Longcope 1999). In Fig. 4 we show the distribution of BP lifetimes over the first quarter of 2000. This distribution appears to be weakly bimodal and we have identified the lifetimes of active region (green Gaussian fitted curve; mean value of 5.2 hours) and quiet-Sun (red Gaussian; mean value of 29.2 hours) BPs.

In Fig. 5 we show the variations of the BP quarterly mean lifetimes (the error bars reflect the deviation of the distributions) from 1996 until the end of 2000. While it appears that the mean quiet-Sun BP lifetimes appear to be fairly constant over this period at ~ 29 hours the active region BP lifetimes appear to decay slightly on the rising phase of cycle 23. We note, however, that the actual downward trend is consistent with a constant value of ~ 6 hours within the error bars. Clearly, we need to continue the analysis and compute BP lifetimes that map out the remainder of cycle 23. It is as yet unclear if this variation is merely a selection effect (e.g., very few active region BPs in 1996) or if it is actually tied to the mechanism that drives the appearance of active regions and magnetic flux turnover and reconnection; the dynamo.

4. CLOSING REMARKS

We have demonstrated a method to automatically detect EUV bright points and applied it to the archive of EIT data from the launch of *SOHO* to the present and is discussed at significantly greater length in McIntosh & Gurnan (2004). In applying this method we have produced a database of all the detected BPs that allow us to track their appearance, in space, time and in three (relatively narrow) temperature regions. There are many fundamental diagnostics of the solar corona over the current solar cycle that are simple byproducts of BP cataloging, those demonstrated above are only a small subset.

4.1 Further Work

Going beyond the relatively small EIT data archive, the impossibility of manual interpretation of the corresponding data expected from Solar Dynamics Observatory (SDO) is manifest: the Atmospheric Imaging Array (AIA) will obtain 4096 x 4096-pixel images in at least six wavelengths likely to show bright points, every ten seconds - [2 x wavelengths * 16 x pixels * 72 x cadence] more than a 2,000-fold increase over the maximum EIT data rate. Fortunately, EIT's eight-plus years of observations provide an invaluable "training set" of data objects that will mimic those of AIA, in particular. The relatively small volume of the *SOHO* image data archive makes it reasonable to develop and implement an automated data analysis agent that is ready for implementation upon the launch of SDO and can yield some guideline results from cycle 23 as benchmark measurements for direct comparison with those of cycle 24. For a limited period of time, the analysis of *SOHO* and SDO EUV data will be coupled and will be entirely complementary provided that that former is still operational. Also, given the increase in the capacity of computing hardware, the *SOHO*/SDO BP database will be updated in real time.

We should note that the EIT BP database will become available on the EIT webpage at GSFC <http://umbra.nascom.nasa.gov/eit/>.

ACKNOWLEDGMENTS

SWM acknowledges the past support of the Solar Data Analysis Center and the Living With A Star program at GSFC.

REFERENCES

- Acton, L., Tsuneta, S., Ogawara, Y., *et al.*, 1992, *Science*, 258, 616
- Brajsa, R., Whl, H., Vrsnak, B., *et al.*, 2001, *A & A*, 374, 309
- Brown, D.S., Parnell, C.E., Deluca, E.E., *et al.*, 2002, *Adv. in Sp. Res.*, 29(7), 1093
- Delaboudinière, J.-P., Artzner, G.E., Brunaud, A.H., *et al.*, 1995, *Sol. Phys.*, 162, 291
- Do, M.N., Vetterli, M., 2003, *IEEE Trans. on Image Proc.*, 12(1), 16
- Fleck, B., Domingo, V., Poland, A.I., 1995, "The *SOHO* Mission", Dordrecht, Kluwer.
- Freeland, S.L., Handy, B.N., 1998, *Sol. Phys.*, 182, 497
- Golub, L., Krieger, A.S., Silk, J.K., *et al.*, 1974, *ApJL*, 189, 93
- Gurman, J.B., 2002, In *Proceedings of the SOHO 11 Symposium: "From Solar Min to Max: Half a Solar Cycle with SOHO"*, Wilson, A. (Ed.), ESA SP-508, 525
- Hara, H., Nakakubo-Morimoto, K., 2003, *ApJ*, 589, 1062
- Harvey, K.L., Strong, K.T., Nitta, N., Tsuneta, S., 1993, *Adv. in Sp. Res.*, 13, 27
- Harvey, K.L., Strong, K.S., Nitta, N., Tsuneta, S., 1994a, In "Solar Active Region Evolution: Comparing Models with Observations". *Astronomical Society of the Pacific Conference Series*, 68, K. S. Balasubramaniam K.S. & Simon, G.W., (Eds.) 377
- Harvey, K.L., Nitta, N., Strong, K.T., Tsuneta, S., 1994b, In "X-ray Solar Physics from Yohkoh", Uchida Y., Watanabe, T., Shibata, K. & Hudson, H.S. (Eds.), 21
- Harvey, K.L., 1997, In "Magnetic Reconnection in the Solar Atmosphere". *ASP Conference Series*; Vol. 111, Bentley R.D. & Mariska J.T. (Eds.), 9
- Kankelborg, C.C., Longcope, D.W., 1999, *Sol. Phys.*, 190, 59
- Newton, H.W. & Nunn, M.L., *MNRAS*, 111, 413
- McIntosh, S.W. & Gurman, J.B., 2005, In preparation to be submitted *ApJ*
- Pawal, P., 1999, *ApJL*, 510, 73
- Sattarov, I., Pevtsov, A.A., Hojaev, A.S., Sherdonov, C.T., 2002, *ApJ*, 564, 1042
- Scherrer, P.H., Bogart, R.S., Bush, R.I., *et al.* 1995, *Sol. Phys.*, 162, 129
- Shimojo, M., Shibata, K., 1999, *ApJ*, 516, 934
- Vaiana, G.S., Krieger, A.S., Timothy, A.F., 1973, *Sol. Phys.*, 32, 81